STANFORD
AERONAUTICS &
ASTRONAUTICS

Similarity Rules for Incompressible Turbulent Shear Flows

Brian Cantwell
Stanford University
May 21, 2025

STANFORD
AERONAUTICS &
ASTRONAUTICS

Incompressible Flow

Symmetries of the Navier Stokes Equations

$$\frac{\partial u^j}{\partial x^j} = 0, \quad \text{(sum over } j = 1, 2, 3),$$

$$\frac{\partial u^i}{\partial t} + u^j \frac{\partial u^i}{\partial x^j} + \frac{\partial p}{\partial x^i} - \nu \frac{\partial^2 u^i}{\partial x^j \partial x^j} = 0, \qquad i = 1, 2, 3, \qquad (11.1)$$

sum over $j = 1, 2, 3$

Infinitesimal transformation

$$\begin{aligned} \tilde{x}^i &= x^i + s\xi^i[\boldsymbol{x}, t], \\ \tilde{t} &= t + s\tau[\boldsymbol{x}, t], \\ \tilde{u}^i &= u^i + s\eta^i[\boldsymbol{x}, t], \\ \tilde{p} &= p + s\zeta[\boldsymbol{x}, t]. \end{aligned}$$

STANFORD AERONAUTICS & ASTRONAUTICS

The equations are invariant under a 9-parameter group of translations, rotations and dilations

(1) Invariance under translation in time:

$$X^1 = \frac{\partial}{\partial t}. \tag{11.3}$$

(2) An arbitrary function of time, $g[t]$, added to the pressure:

$$X^2 = g[t]\frac{\partial}{\partial p}. \tag{11.4}$$

(3) Rotation about the z-axis:

$$X^3 = y\frac{\partial}{\partial x} - x\frac{\partial}{\partial y} + v\frac{\partial}{\partial u} - u\frac{\partial}{\partial v}. \tag{11.5}$$

(4) Rotation about the x-axis:

$$X^4 = z\frac{\partial}{\partial y} - y\frac{\partial}{\partial z} + w\frac{\partial}{\partial v} - v\frac{\partial}{\partial w}. \tag{11.6}$$

(5) Rotation about the y-axis:

$$X^5 = z\frac{\partial}{\partial x} - x\frac{\partial}{\partial z} + w\frac{\partial}{\partial u} - u\frac{\partial}{\partial w}. \tag{11.7}$$

(6) Nonuniform translation in the x-direction:

$$X^6 = a[t]\frac{\partial}{\partial x} + \left(\frac{da}{dt}\right)\frac{\partial}{\partial u} - x\left(\frac{d^2a}{dt^2}\right)\frac{\partial}{\partial p}. \tag{11.8}$$

$a[t]$ is an arbitrary, twice differentiable function of time. Simple translation in x corresponds to $a[t] = \text{const}$.

(7) Nonuniform translation in the y-direction:

$$X^7 = b[t]\frac{\partial}{\partial y} + \left(\frac{db}{dt}\right)\frac{\partial}{\partial v} - y\left(\frac{d^2b}{dt^2}\right)\frac{\partial}{\partial p}. \tag{11.9}$$

$b[t]$ is an arbitrary, twice differentiable function.

(8) Nonuniform translation in the z-direction:

$$X^8 = c[t]\frac{\partial}{\partial z} + \left(\frac{dc}{dt}\right)\frac{\partial}{\partial w} - z\left(\frac{d^2c}{dt^2}\right)\frac{\partial}{\partial p}. \tag{11.10}$$

$c[t]$ is an arbitrary, twice differentiable function.

(9) The one-parameter dilation group of the equation

$$X^9 = 2t\frac{\partial}{\partial t} + x\frac{\partial}{\partial x} + y\frac{\partial}{\partial y} + z\frac{\partial}{\partial z} - u\frac{\partial}{\partial u} - v\frac{\partial}{\partial v} - w\frac{\partial}{\partial w} - 2p\frac{\partial}{\partial p}. \tag{11.11}$$

STANFORD
AERONAUTICS &
ASTRONAUTICS

One-parameter dilation group of the full viscous equations.

$$\tilde{x}^i = e^s x^i,$$
$$\tilde{t} = e^{2s} t,$$
$$\tilde{u}^i = e^{-s} u^i,$$
$$\tilde{p} = e^{-2s} p.$$

If the kinematic viscosity is set to zero, the resulting Euler equations are invariant under a two-parameter dilation group.

$$\tilde{x}^i = e^s x^i,$$
$$\tilde{t} = e^{s/k} t,$$
$$\tilde{u}^i = e^{s(1-1/k)} u^i,$$
$$\tilde{p} = e^{s(2-2/k)} p$$

The Euler equations are invariant for any value of k.

STANFORD
AERONAUTICS &
ASTRONAUTICS

In addition, the equations are invariant under a group of arbitrary translations in space.

$$\tilde{x}^j = x^j + a^j[t],$$
$$\tilde{t} = t,$$
$$\tilde{u}^i = u^i + \frac{da^i}{dt},$$
$$\tilde{p} = p - x^j \frac{d^2 a^j}{dt^2} + g[t].$$

STANFORD
AERONAUTICS &
ASTRONAUTICS

Instantaneous flow field in the wake of a circular cylinder as seen by two observers (again!).

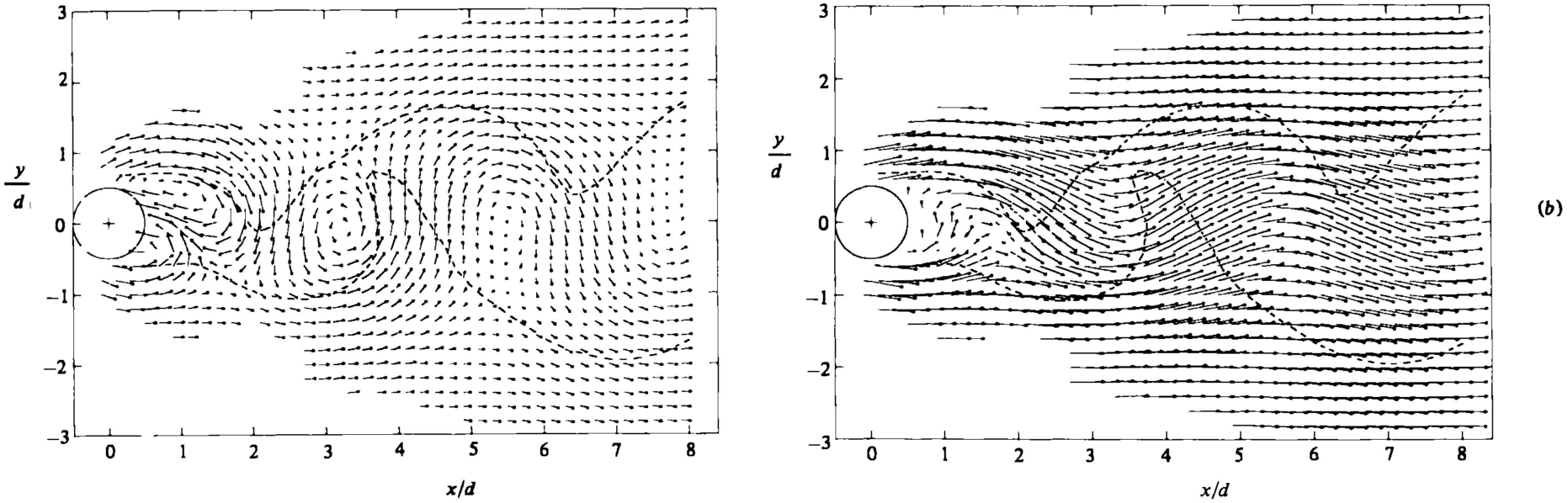

FIGURE 20. Interpolated velocity field at constant phase (7, 15) over 8 diameters of the wake as viewed from a frame of reference (*a*) moving downstream at $0.755u_\infty$, (*b*) fixed with respect to the cylinder. Dashed line is contour $\langle\gamma\rangle = 0.5$ from figure 23(*b*).

STANFORD
AERONAUTICS &
ASTRONAUTICS

Reynolds Number Invariance

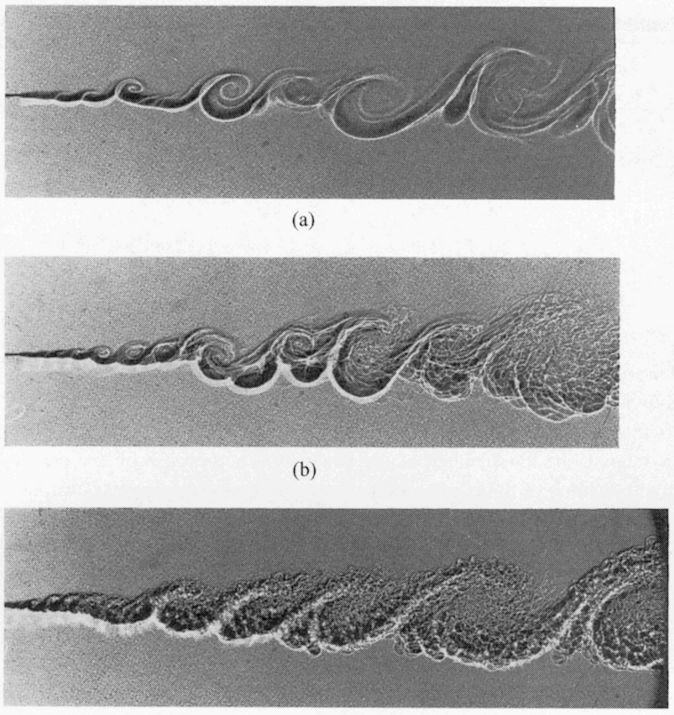

Fig. 13.1. Effects of Reynolds number on a plane mixing layer between helium (upper stream) and nitrogen (lower stream) from Brown and Roshko [13.1] and Roshko[13.2]. The Reynolds number in (a) is approximately 1.3×10^4 centimeter^{-1}. The thickness of the layer at the right side of the picture is approximately 2 cm. The speed of the lower stream is 10 m/s. Test-section pressures in atmospheres are: (a) 2, (b) 4, (c) 8. Dynamic pressures in the upper and lower streams are the same: $\rho_1 u_1^2 = \rho_2 u_2^2$.

STANFORD
AERONAUTICS &
ASTRONAUTICS

The Reynolds averaged Navier-Stokes equations

$$\boldsymbol{u} = \bar{\boldsymbol{u}} + \boldsymbol{u}', \qquad p = \bar{p} + p', \tag{13.1}$$

$$\begin{aligned} \frac{\partial \bar{u}^i}{\partial x^i} &= 0, \\ \frac{\partial \bar{u}^i}{\partial t} + \frac{\partial}{\partial x^j}(\bar{u}^j \bar{u}^i) + \frac{1}{\rho}\frac{\partial \bar{p}}{\partial x^i} - \frac{1}{\rho}\frac{\partial \tau^{ij}}{\partial x^j} - 2\nu\frac{\partial \bar{s}^{ij}}{\partial x^j} &= 0, \end{aligned} \tag{13.2}$$

Rate-of-strain $$\bar{s}^{ij} = \frac{1}{2}\left(\frac{\partial \bar{u}^i}{\partial x^j} + \frac{\partial \bar{u}^j}{\partial x^i}\right). \tag{13.3}$$

$$\frac{\tau^{ij}}{\rho} = -\overline{u'^i u'^j}. \tag{13.4}$$

Away from a wall $$-\overline{u'^i u'^j} \gg 2\nu \bar{s}^{ij}. \tag{13.5}$$

For free shear flows the viscous stresses are often neglected compared to the Reynolds stresses.

$$\begin{aligned} \frac{\partial \bar{u}^j}{\partial x^j} &= 0, \\ \frac{\partial \bar{u}^i}{\partial t} + \frac{\partial}{\partial x^j}(\bar{u}^j \bar{u}^i) + \frac{1}{\rho}\frac{\partial \bar{p}}{\partial x^i} - \frac{1}{\rho}\frac{\partial \tau^{ij}}{\partial x^j} &= 0. \end{aligned} \tag{13.6}$$

STANFORD AERONAUTICS & ASTRONAUTICS

Integral length and velocity scales

u_0 = integral velocity scale characterizing the overall motion,
δ = integral length scale characterizing the overall motion.

Turbulent Kinetic Energy TKE

$$u' = \sqrt{\frac{u_1'^2 + u_2'^2 + u_3'^2}{2}}. \tag{13.7}$$

$$u' \propto u_0, \tag{13.8}$$

Viscous dissipation of TKE

$$\varepsilon = 2\nu \overline{s'^{ij} s'^{ji}}, \tag{13.9}$$

$$s'^{ij} = \frac{1}{2}\left(\frac{\partial u'^i}{\partial x^j} + \frac{\partial u'^j}{\partial x^i}\right) \tag{13.10}$$

Dissipation of TKE scales with production of TKE

$$\varepsilon \propto \overline{u'^i u'^j} \frac{\partial \bar{u}^i}{\partial x^j}. \tag{13.11}$$

$$\varepsilon \propto \frac{u_0^3}{\delta}. \tag{13.12}$$

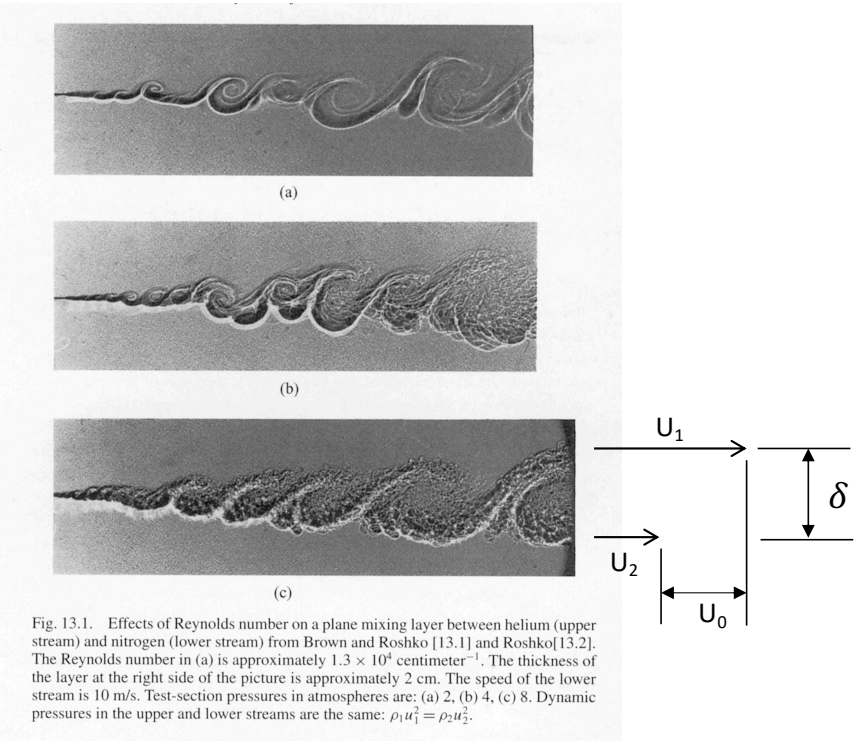

Fig. 13.1. Effects of Reynolds number on a plane mixing layer between helium (upper stream) and nitrogen (lower stream) from Brown and Roshko [13.1] and Roshko[13.2]. The Reynolds number in (a) is approximately 1.3×10^4 centimeter^{-1}. The thickness of the layer at the right side of the picture is approximately 2 cm. The speed of the lower stream is 10 m/s. Test-section pressures in atmospheres are: (a) 2, (b) 4, (c) 8. Dynamic pressures in the upper and lower streams are the same: $\rho_1 u_1^2 = \rho_2 u_2^2$.

STANFORD
AERONAUTICS &
ASTRONAUTICS

Invariant group of the Euler equations

$$\tilde{x}^i = e^s x^i, \qquad \tilde{t} = e^{s/k} t, \qquad \tilde{\bar{u}}^i = e^{s(1-1/k)} \bar{u}^i,$$
$$\tilde{\tau}^{ij} = e^{s(2-2/k)} \tau^{ij}, \qquad \tilde{\bar{p}} = e^{s(2-2/k)} \bar{p}, \tag{13.13}$$

$$\frac{\partial \tilde{\bar{u}}^i}{\partial \tilde{t}} + \frac{\partial}{\partial \tilde{x}^j} \tilde{\bar{u}}^j \tilde{\bar{u}}^i + \frac{\partial \tilde{\bar{p}}}{\partial \tilde{x}^i} - \frac{\partial \tilde{\tau}^{ij}}{\partial \tilde{x}^j}$$
$$= \left(\frac{\partial \bar{u}^i}{\partial t} + \frac{\partial}{\partial x^j} \bar{u}^j \bar{u}^i + \frac{\partial \bar{p}}{\partial x^i} - \frac{\partial \tau^{ij}}{\partial x^j} \right) e^{a(1-2/k)} = 0. \tag{13.14}$$

STANFORD AERONAUTICS & ASTRONAUTICS

One parameter flows

$$\hat{M} = L^m T^{-n} \qquad \widehat{\ } \text{ "units of"} \qquad (13.15)$$

Stationary plane jet. The integral momentum flux J/ρ is approximately constant at any streamwise position:

$\widehat{M} = \mathsf{L}^3/\mathsf{T}^2$

$$\frac{J}{\rho} = \int_{-\infty}^{\infty} \tilde{u}^2 \, d\tilde{y} = e^{a(3-2/k)} \int_{-\infty}^{\infty} u^2 \, dy.$$

The integral is invariant under dilation only for $k = \frac{2}{3}$.

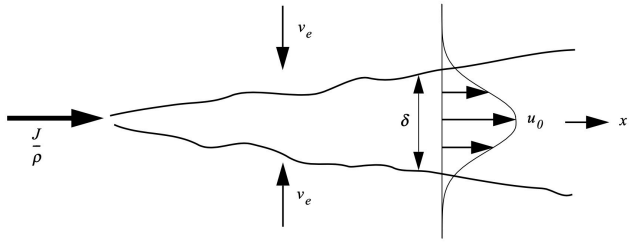

Vortex ring. The hydrodynamic impulse, I/ρ, is the conserved integral for this flow (cf. Chapter 11, Section 11.5.1):

$\widehat{M} = \mathsf{L}^4/\mathsf{T}$

$$\frac{I}{\rho} = \frac{3}{2} \int \tilde{u} \, d\tilde{x} \, d\tilde{y} \, d\tilde{z} = e^{a(4-1/k)} \frac{3}{2} \int u \, dx \, dy \, dz.$$

In this case the integral is invariant for $k = \frac{1}{4}$.

STANFORD AERONAUTICS & ASTRONAUTICS

Temporal similarity rules

$$\frac{dx^i}{x^i} = k\frac{dt}{t} = \left(\frac{k}{k-1}\right)\frac{du^i}{u^i} = \left(\frac{k}{2k-2}\right)\frac{dp}{p} = \left(\frac{k}{2k-2}\right)\frac{d\tau^{ij}}{\tau^{ij}} \quad (13.18)$$

$$\xi^i = \frac{x^i}{\delta[t]}, \qquad U^i = \frac{u^i}{u_0[t]}, \qquad P = \frac{p}{u_0[t]^2}, \qquad T^{ij} = \frac{\tau^{ij}}{u_0[t]^2}. \quad (13.19)$$

The time-dependent length and velocity scales in (13.19) are

$$\boxed{\delta[t] \propto M^{1/m}(t-t_0)^k, \qquad u_0[t] \propto M^{1/m}(t-t_0)^{k-1},} \quad (13.20)$$

$$\hat{M} = L^m T^{-n}$$

where t_0 is the effective origin in time. The group parameter k is determined by the units of the governing parameter M:

$$\boxed{k = n/m.} \quad (13.21)$$

$$\frac{u^i}{u_0[t]} = U^i\left[\frac{\boldsymbol{x}}{\delta[t]}\right], \qquad \frac{p}{u_0[t]^2} = P\left[\frac{\boldsymbol{x}}{\delta[t]}\right], \qquad \frac{\tau^{ij}}{u_0[t]^2} = T^{ij}\left[\frac{\boldsymbol{x}}{\delta[t]}\right]. \quad (13.22)$$

STANFORD
AERONAUTICS &
ASTRONAUTICS

Reduced equations

When the similarity variables (13.22) are substituted into the Reynolds equations (13.2), the result is that time drops out of the equations and the number of independent variables is reduced from four to three:

$$\frac{\partial U^j}{\partial \xi^j} = 0,$$

$$(k-1)U^i + (U^j - k\xi^j)\frac{\partial U^i}{\partial \xi^j} + \frac{1}{\rho}\frac{\partial P}{\partial \xi^i} - \frac{1}{\rho}\frac{\partial}{\partial \xi^j}(T^{ij}) = 0. \quad (13.23)$$

The equations for particle paths,

$$\frac{dx^i}{dt} = u^i[\boldsymbol{x}, t], \quad (13.24)$$

transform to the autonomous system

$$\frac{d\xi^i}{d\tau} = U^i[\boldsymbol{\xi}] - k\xi^i. \quad (13.25)$$

In these one-parameter flows all lengths scale with the same power of time enabling the basic time dependence of the flow to be incorporated into space-time similarity variables.

Derivation of 13.25

$$\frac{dx^i}{dt} = u^i$$

$$\xi^i = \frac{x^i}{M^{1/m}(t-t_0)^k}$$

$$dx^i = M^{1/m}(t-t_0)^k d\xi^i + k\xi^i M^{1/m}(t-t_0)^{k-1}dt$$

$$M^{1/m}(t-t_0)^k\frac{d\xi^i}{dt} + k\xi^i M^{1/m}(t-t_0)^{k-1} = M^{1/m}(t-t_0)^{k-1}U^i$$

$$(t-t_0)\frac{d\xi^i}{dt} + k\xi^i = U^i$$

$$\frac{d\xi^i}{d\tau} = U^i - k\xi^i$$

$$\tau = ln(t-t_0)$$

STANFORD
AERONAUTICS &
ASTRONAUTICS

Frames of reference

If an observer is selected to convect with a particular feature of the flow, then the observer will have to translate nonuniformly according to the power of time appropriate to the flow. Such a transformation is defined by

$$\begin{aligned} \tilde{x}^i &= x^i - \alpha^i M^{1/m}(t-t_0)^k, \\ \tilde{t} &= t, \\ \tilde{\bar{u}}^i &= \bar{u}^i - k\alpha^i M^{1/m}(t-t_0)^{k-1}, \\ \tilde{\bar{p}} &= \bar{p} + x^j k(k-1)\alpha^j M^{1/m}(t-t_0)^{k-2}, \end{aligned} \tag{13.26}$$

where the α^i determine the relative rates of motion of the observer in the three directions. We already know from the discussion in Chapter 11, Section 11.2, that the Navier–Stokes and Euler equations are invariant under the group (13.26). The Reynolds equations with the viscous term removed, (13.6), are as well. In terms of similarity variables, (13.26) becomes a simple translation,

$$\begin{aligned} \tilde{\xi}^i &= \xi^i - \alpha^i, \\ \tilde{\tau} &= \tau, \\ \tilde{U}^i &= U^i - k\alpha^i, \\ \tilde{P} &= P + \alpha^j \xi^j k(k-1). \end{aligned} \tag{13.27}$$

In similarity coordinates, the equations for particle paths transform as follows:

$$\begin{aligned} \frac{d\tilde{\xi}^i}{d\tilde{\tau}} &= \frac{d\xi^i}{d\tau}, \\ \tilde{U}^i[\tilde{\boldsymbol{\xi}}] - k\tilde{\xi}^i &= U^i[\boldsymbol{\xi}] - k\xi^i. \end{aligned} \tag{13.28}$$

The vector field of particle paths in similarity coordinates is independent of the observer.

STANFORD
AERONAUTICS & ASTRONAUTICS

Spatial similarity rules - jets

All turbulent one-parameter jets spread linearly in space

2D jets
$\widehat{M}$ = L³ / T², k=2/3

3D jets
$\widehat{M}$ = L⁴ / T², k=1/2

$$(x - x_0) \propto M^{1/m}(t - t_0)^k. \qquad (13.29)$$

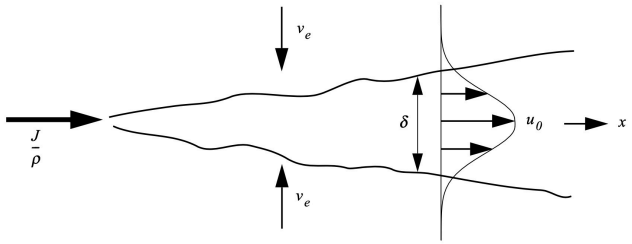

$$\delta \propto (x - x_0), \qquad u_0 \propto M^{1/n}(x - x_0)^{1-1/k}. \qquad (13.30)$$

Spatial similarity rules - wakes

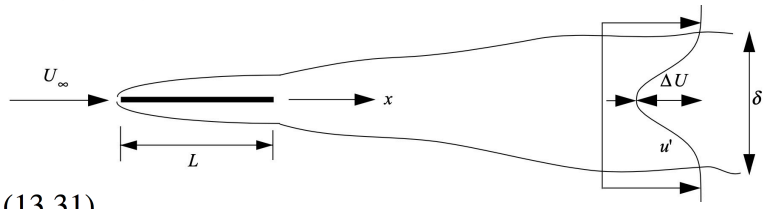

$$\frac{D}{\rho} = C_D\left(\frac{1}{2}U_\infty^2\right)(\pi R^2). \qquad (13.31)$$

2D wakes
$\widehat{M}$ = L² / T, k=1/2

3D wakes
$\widehat{M}$ = L³ / T, k=1/3

$$\frac{D}{\rho} \propto \int_A U(U_\infty - U)\, dA, \qquad (13.32)$$

$$\frac{D}{\rho U_\infty} \propto \int_A (U_\infty - U)\, dA. \qquad (13.33)$$

$$(x - x_0) = U_\infty(t - t_0). \qquad (13.34)$$

$$\delta \propto M^{1/m}U_\infty^{-k}(x - x_0)^k, \qquad u_0 \propto M^{1/m}U_\infty^{1-k}(x - x_0)^{k-1}. \qquad (13.35)$$

Even flows where the initial region may be dominated by several length scales, as is the case with the origins of jets and wakes, the downstream region generally follows the scaling of a single governing parameter.

If k > 1/2 the range of scales increases continuously.

If k = 1/2 the range of scales is constant.

If k < 1/2 the range of scales decreases, and viscosity eventually dominates the motion.

STANFORD
AERONAUTICS &
ASTRONAUTICS

Reynolds number scaling

$$R_\delta = \frac{U_0 \delta}{\nu} \propto \frac{M^{2/m}}{\nu}(t - t_0)^{2k-1}. \qquad (13.36)$$

If k > ½, R_δ increases with time – the ratio of large to small eddy length scales increases

If k = ½, R_δ is constant independent of space and time

If k < ½, R_δ decreases with time – the flow relaminaries

The idea of an eddy viscosity

$$-\overline{u'v'} = \nu_\tau \frac{\partial \bar{u}}{\partial y}. \qquad (13.37)$$

$$\nu_\tau \propto u_0\, \delta. \qquad (13.38)$$

$$Re_\tau = \frac{u_0 \delta}{\nu_\tau} \propto \text{constant} \qquad (13.39)$$

Table 13.1. *Various one-parameter shear flows and the units of the associated governing parameter.*

Flow	Invariant	M	Units	k
	Jetlike flows			
Plane mixing layer	Velocity difference	U_0	LT^{-1}	1
Plane jet	2-D momentum flux	$U_0^2\delta$	L^3T^{-2}	$\frac{2}{3}$
Round jet	3-D momentum flux	$U_0^2\delta^2$	L^4T^{-2}	$\frac{1}{2}$
Radial jet	3-D momentum flux	$U_0^2\delta^2$	L^4T^{-2}	$\frac{1}{2}$
Vortex pair	2-D impulse	$U_0\delta^2$	L^3T^{-1}	$\frac{1}{3}$
Vortex ring	3-D impulse	$U_0\delta^3$	L^4T^{-1}	$\frac{1}{4}$
Plane plume	2-D buoyancy flux	U_0^3	L^3T^{-3}	1
Round plume	3-D buoyancy flux	$U_0^3\delta$	L^4T^{-3}	$\frac{3}{4}$
Plane thermal	2-D buoyancy	$U_0^2\delta$	L^3T^{-2}	$\frac{2}{3}$
Round thermal	3-D buoyancy	$U_0^2\delta^2$	L^4T^{-2}	$\frac{1}{2}$
Line vortex	Circulation	$U_0\delta$	L^2T^{-1}	$\frac{1}{2}$
Diverging channel	Area flux	$U_0\delta$	L^2T^{-1}	$\frac{1}{2}$
Vortex-sheet rollup	Apex α; $n = 1/(2-\alpha/\pi)$	$U_0^2\delta^{2-n}$	$L^{3-n}T^{-1}$	$1/(3-n)$
	Wakelike flows			
Plane wake	(2-D drag)$/U_\infty$	$U_0\delta$	L^2T^{-1}	$\frac{1}{2}$
Round wake	(3-D drag)$/U_\infty$	$U_0\delta^2$	L^3T^{-1}	$\frac{1}{3}$
Plane jet in cross flow	(2-D mom. flux)$/U_\infty$	$U_0\delta$	L^2T^{-1}	$\frac{1}{2}$
Round jet in cross flow	(3-D mom. flux)$/U_\infty$	$U_0\delta^2$	L^3T^{-1}	$\frac{1}{3}$
Plane plume in cross flow	(2-D buoy. flux)$/U_\infty$	U_0^2	L^2T^{-2}	1
Round plume in cross flow	(3-D buoy. flux)$/U_\infty$	$U_0^2\delta$	L^3T^{-2}	$\frac{2}{3}$
Grid turb. initial decay	Saffman invariant	$U_0^2\delta^3$	L^5T^{-2}	$\frac{2}{5}$
Grid turb. initial decay	Loitsianski invariant	$U_0^2\delta^5$	L^7T^{-2}	$\frac{2}{7}$

STANFORD
AERONAUTICS &
ASTRONAUTICS

Growth of a turbulent vortex ring

The governing parameter is the hydrodynamic impulse $\frac{\hat{I}}{\rho} = \frac{L^4}{T^2}$, $k = \frac{1}{4}$

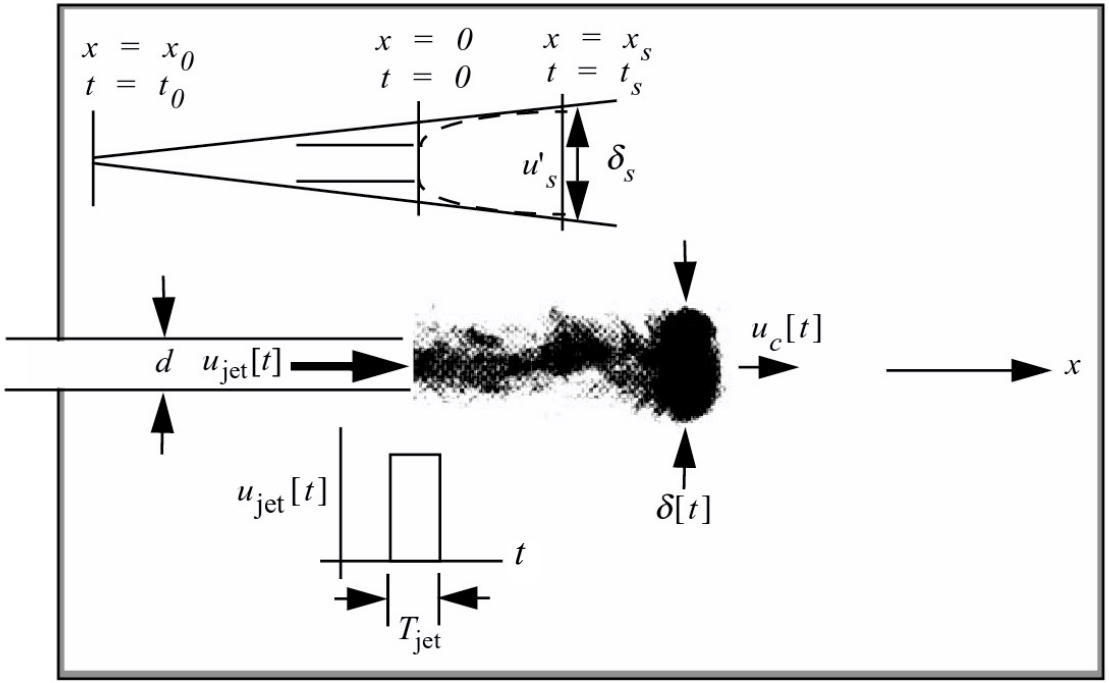

Fig. 13.3. Vortex-ring apparatus with experimental parameters. The sketch in the upper part of the figure defines parameters used to determine the effective origin of the ring.

STANFORD
AERONAUTICS &
ASTRONAUTICS

High and Low Reynolds number vortex rings

(a)

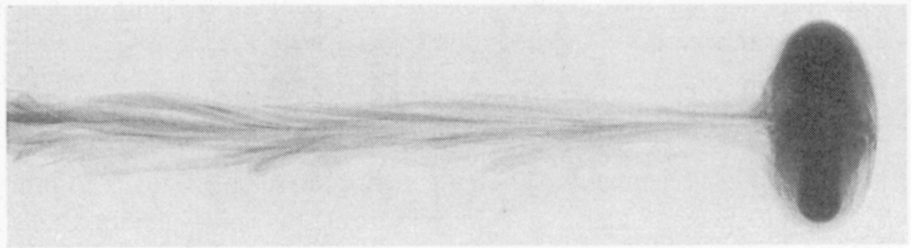

(b)

Fig. 13.2. Turbulent and laminar vortex rings produced by an impulsive force, from the paper by Glezer and Coles [13.17]. Initial Reynolds number Γ_0/ν is (a) 27,000, (b) 7,500.

STANFORD AERONAUTICS & ASTRONAUTICS

Integral of the motion - the hydrodynamic impulse

$$\frac{3}{2}\int_V u\,dx\,dy\,dz = \int_0^t \int_V \frac{I}{\rho}\delta[x]\delta[y]\delta[z]\delta[t]\,dx\,dy\,dz\,dt = \frac{I}{\rho}, \qquad L^4T^{-1},\ k = 1/4$$

$$\delta[t] \propto (I/\rho)^{1/4}(t-t_0)^{1/4}, \qquad u_0[t] \propto (I/\rho)^{1/4}(t-t_0)^{-3/4},$$

$$\tilde{x}^i = e^a x^i, \qquad \tilde{t} = e^{4a}t, \qquad \tilde{u}^i = e^{-3a}u^i,$$
$$\tilde{\tau}^{ij} = e^{-6a}\tau^{ij}, \qquad \tilde{p} = e^{-6a}p.$$

$$\frac{U^i}{(I/\rho)^{1/4}(t-t_0)^{-3/4}} = G\left[\frac{\boldsymbol{x}-\boldsymbol{x}_0}{(I/\rho)^{1/4}(t-t_0)^{1/4}}\right].$$

$$\xi = \frac{x-x_0}{(I/\rho)^{1/4}(t-t_0)^{1/4}}, \qquad \eta = \frac{y}{(I/\rho)^{1/4}(t-t_0)^{1/4}}$$

STANFORD
AERONAUTICS &
ASTRONAUTICS

Experimentally Determined Streamlines and Particle Paths

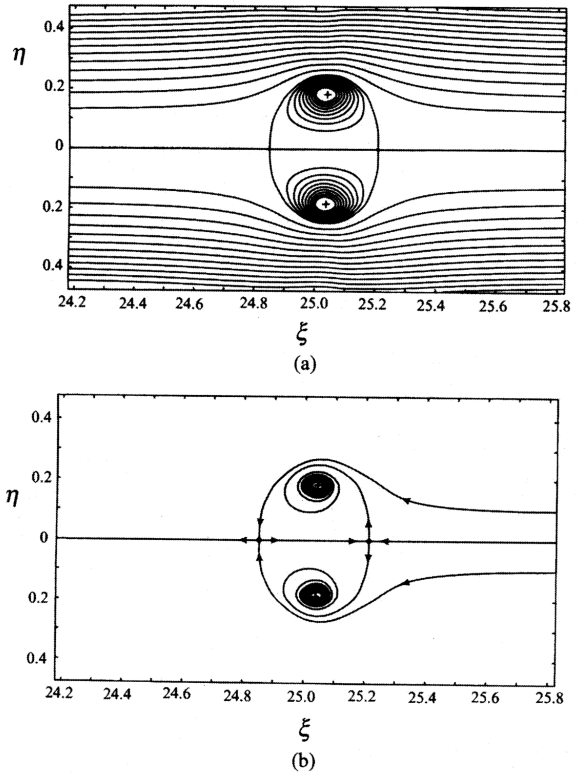

Fig. 13.4. Experimental results from [13.17]: (a) streamline pattern of the ensemble mean velocity field referred to an observer translating to the right with the ring, (b) particle paths of the ensemble mean velocity field.

STANFORD
AERONAUTICS &
ASTRONAUTICS

Recall that the incompressible Navier-Stokes equations are invariant under a group of arbitrary translations in space.

$$\tilde{x}^j = x^j + a^j[t],$$
$$\tilde{t} = t,$$
$$\tilde{u}^i = u^i + \frac{da^i}{dt},$$
$$\tilde{p} = p - x^j \frac{d^2 a^j}{dt^2} + g[t].$$

STANFORD
AERONAUTICS &
ASTRONAUTICS

Reduced equations

$$\frac{\partial U^j}{\partial \xi^j} = 0,$$

$$(k-1)U^i + (U^j - k\xi^j)\frac{\partial U^i}{\partial \xi^j} + \frac{1}{\rho}\frac{\partial P}{\partial \xi^i} - \frac{1}{\rho}\frac{\partial}{\partial \xi^j}(T^{ij}) = 0.$$

Particle paths

$$\frac{dx^i}{dt} = u^i[\boldsymbol{x}, t],$$

$$\frac{d\xi^i}{d\tau} = U^i[\boldsymbol{\xi}] - k\xi^i.$$

Frames of reference

$$\begin{aligned}
\tilde{x}^i &= x^i - \alpha^i M^{1/m}(t - t_0)^k, \\
\tilde{t} &= t, \\
\tilde{u}^i &= u^i - k\alpha^i M^{1/m}(t - t_0)^{k-1}, \\
\tilde{p} &= p + x^j k(k-1)\alpha^j M^{1/m}(t - t_0)^{k-2},
\end{aligned}$$

STANFORD
AERONAUTICS &
ASTRONAUTICS

Particle paths in similarity coordinates do not depend on the observer

$$\tilde{\xi}^i = \xi^i - \alpha^i,$$
$$\tilde{\tau} = \tau,$$
$$\tilde{U}^i = U^i - k\alpha^i,$$
$$\tilde{P} = P + \alpha^j \xi^j k(k-1).$$

$$\frac{d\tilde{\xi}^i}{d\tilde{\tau}} = \frac{d\xi^i}{d\tau},$$
$$\tilde{U}^i[\tilde{\boldsymbol{\xi}}] - k\tilde{\xi}^i = U^i[\boldsymbol{\xi}] - k\xi^i.$$

Streamlines and Particle Paths - again

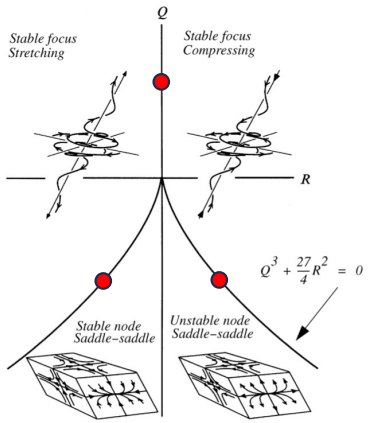

Fig. 3.9. Three-dimensional flow patterns in the plane $P = 0$ (from Reference [3.11]).

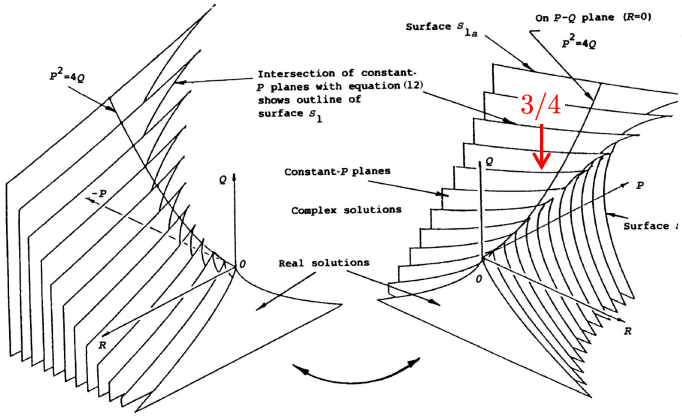

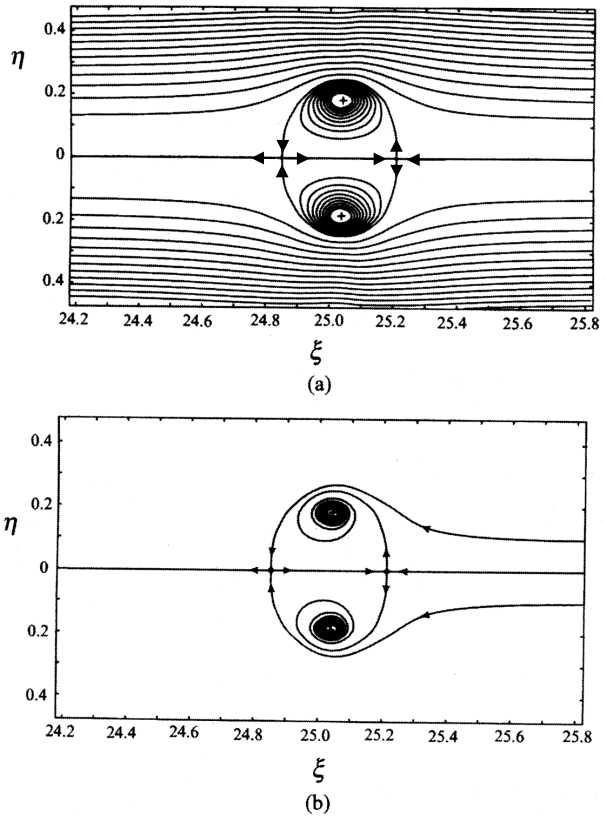

Fig. 13.4. Experimental results from [13.17]: (a) streamline pattern of the ensemble mean velocity field referred to an observer translating to the right with the ring, (b) particle paths of the ensemble mean velocity field.

Critical points are 3D centers and saddles

$$\frac{\partial U^i(\boldsymbol{\xi})}{\partial \xi^i} = 0 \qquad P = 0$$

Critical points are 3D foci and saddles

The particle path plot shows how the vortex ring grows by entraining fluid.

$$\frac{\partial \left(U^i(\boldsymbol{\xi}) - \xi^i/4\right)}{\partial \xi^i} = 0 \qquad P = 3/4$$

STANFORD
AERONAUTICS &
ASTRONAUTICS

Boundary Layer Transition to Turbulence – Turbulent Spots

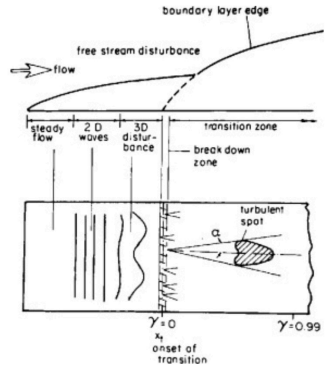

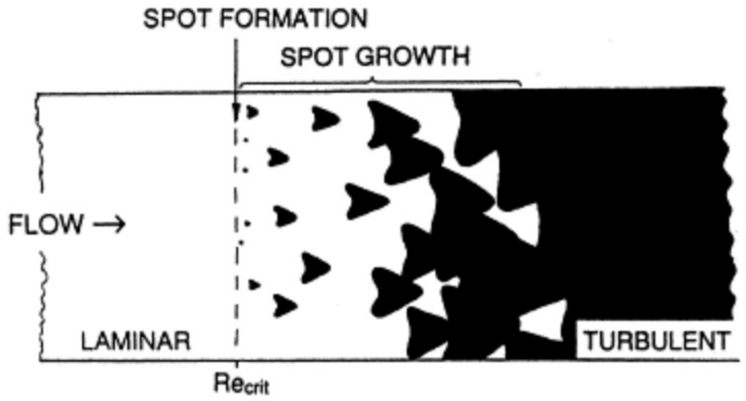

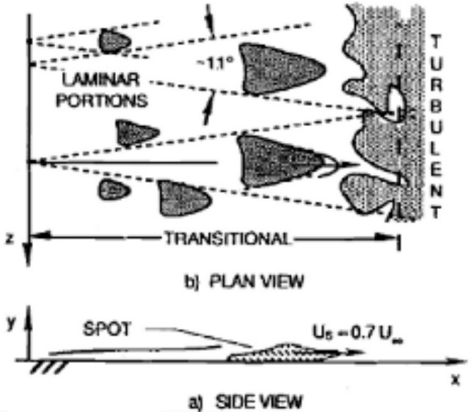

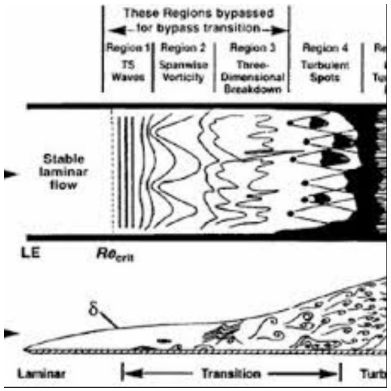

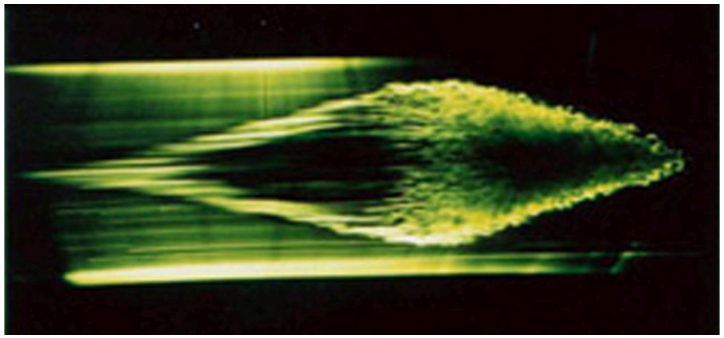

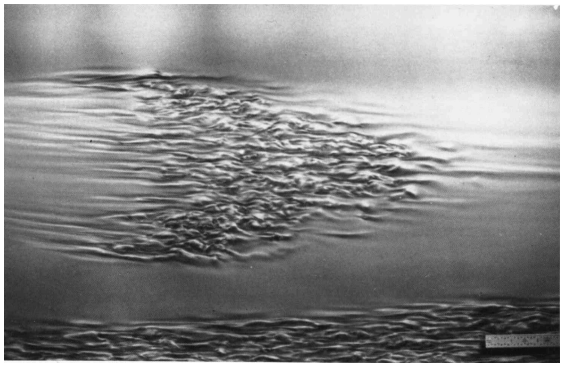

STANFORD
AERONAUTICS &
ASTRONAUTICS

Growth of a Turbulent Spot, $M = U_\infty$, $k = 1$

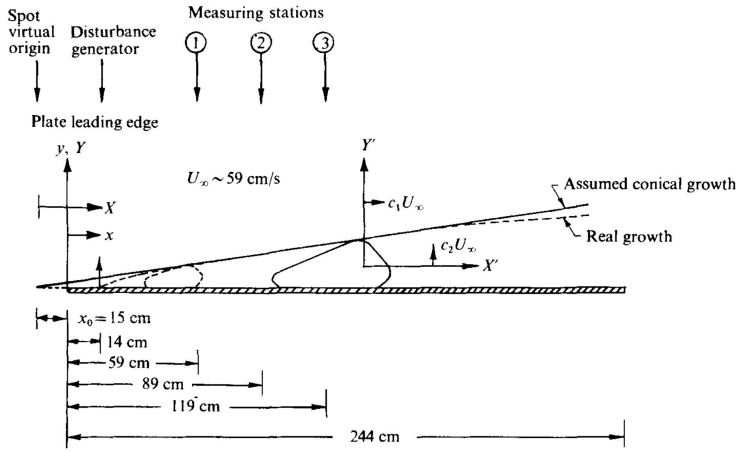

FIGURE 1. Sketch of flat-plate model, showing important dimensions and co-ordinate systems.

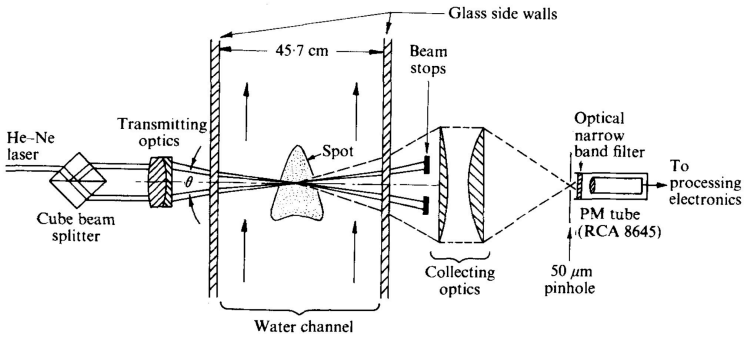

FIGURE 8. Arrangement of transmitting and receiving optics for laser-Doppler velocimetry (not drawn to scale).

Critical points are two sets of foci and saddles one in the outer flow and one near the wall.

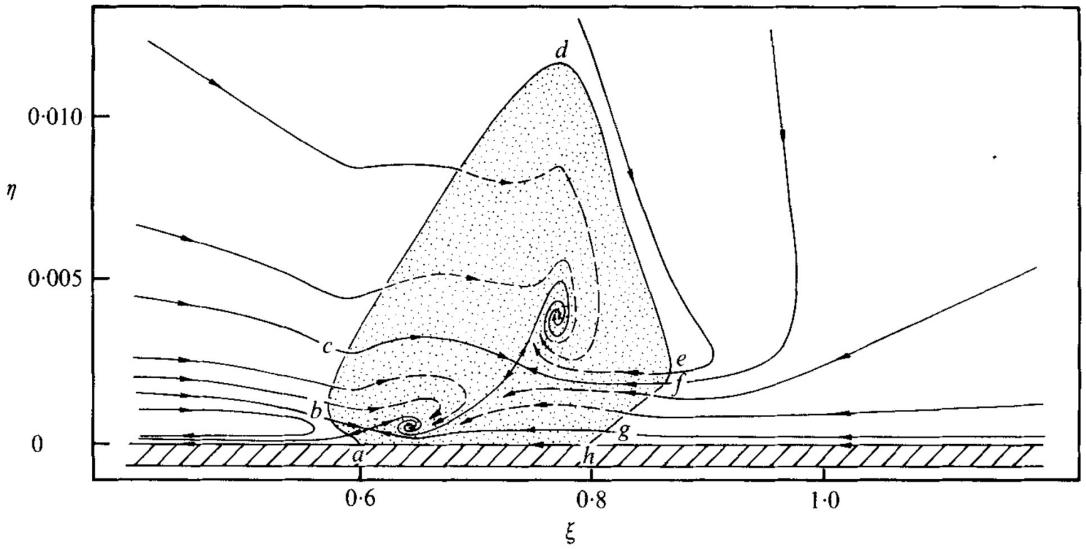

FIGURE 21. Sketch of particle trajectories, with critical points located and classified from the data.

STANFORD
AERONAUTICS &
ASTRONAUTICS

Turbulent Spot Critical Points in (P,Q) space

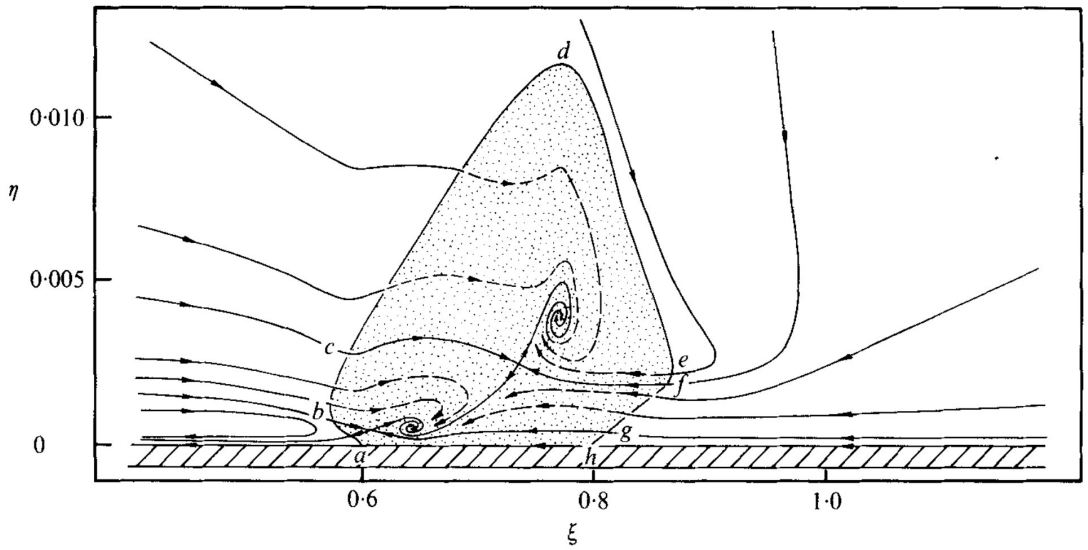

FIGURE 21. Sketch of particle trajectories, with critical points located and classified from the data.

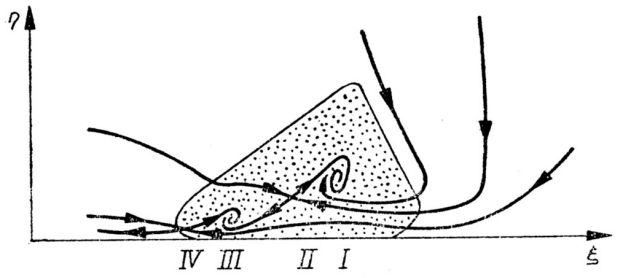

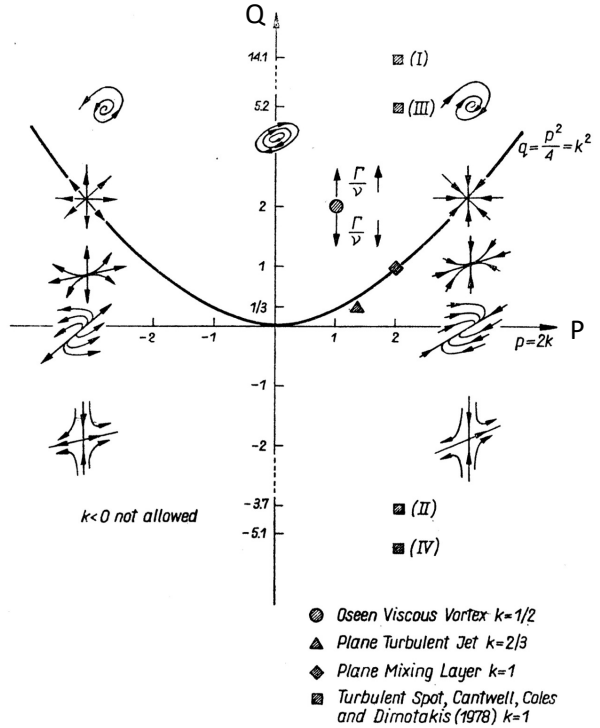

STANFORD
AERONAUTICS &
ASTRONAUTICS

What about fine scales?

First some examples

STANFORD
AERONAUTICS &
ASTRONAUTICS

Instantaneous flow field in the wake of a circular cylinder with contours of TKE production

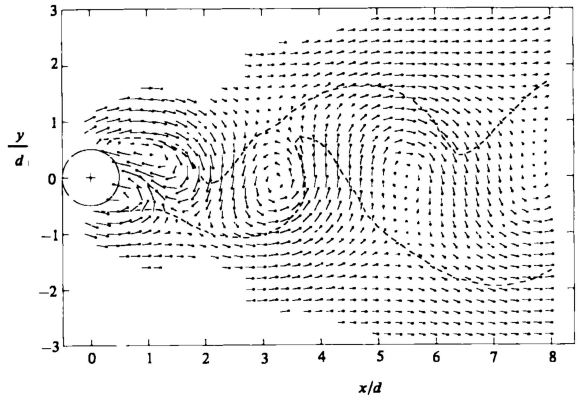

(a)

FIGURE 20. Interpolated velocity field at constant phase (7, 15) over 8 diameters of the wake as viewed from a frame of reference (a) moving downstream at $0.755u_\infty$, (b) fixed with respect to the cylinder. Dashed line is contour $\langle\gamma\rangle = 0.5$ from figure 23(b).

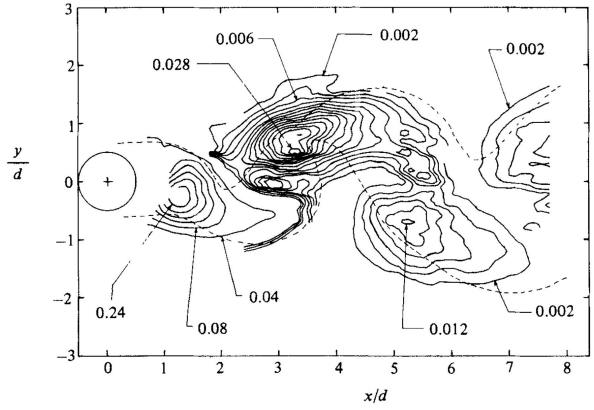

(b)

FIGURE 31. Contours for mean turbulent-energy production. (a) $\overline{P}$, global mean (contour interval 0.010); (b) $\langle P\rangle$, mean at constant phase (7, 15). Note that the range of contour values is greater than 100:1. Contour interval is 0.040 for $x/d \gtrsim 2$; contour interval is 0.002 for $x/d > 2$. Dashed line is contour $\langle\gamma\rangle = 0.5$.

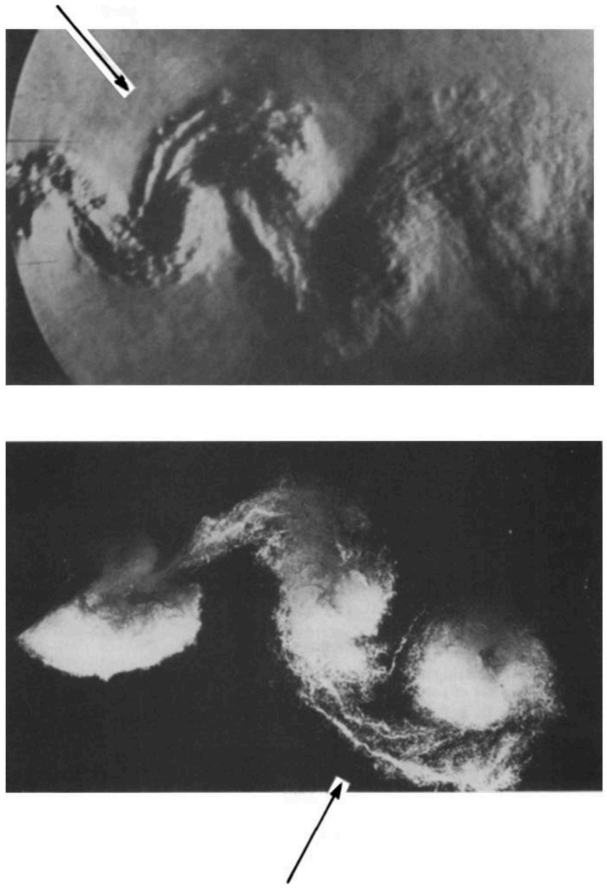

(a)

(b)

FIGURE 32. Visual evidence for organized structure in the saddle region between vortices: (a) near wake of a wedge at $M_\infty = 0.5$ (from Thomann 1959); (b) near wake of a cavitating flapped hydrofoil (from Meijer 1965).

STANFORD
AERONAUTICS &
ASTRONAUTICS

Plane Mixing Layer - Recall integral length and velocity scales

$u_0 =$ integral velocity scale characterizing the overall motion,
$\delta =$ integral length scale characterizing the overall motion.

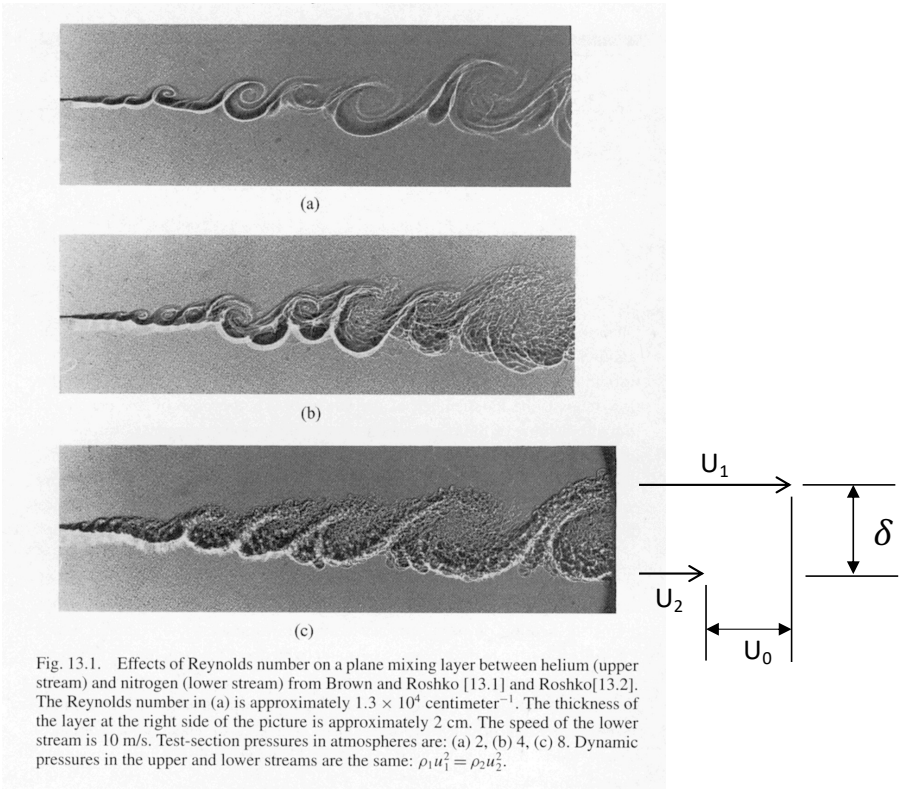

Fig. 13.1. Effects of Reynolds number on a plane mixing layer between helium (upper stream) and nitrogen (lower stream) from Brown and Roshko [13.1] and Roshko[13.2]. The Reynolds number in (a) is approximately 1.3×10^4 centimeter^{-1}. The thickness of the layer at the right side of the picture is approximately 2 cm. The speed of the lower stream is 10 m/s. Test-section pressures in atmospheres are: (a) 2, (b) 4, (c) 8. Dynamic pressures in the upper and lower streams are the same: $\rho_1 u_1^2 = \rho_2 u_2^2$.

STANFORD
AERONAUTICS &
ASTRONAUTICS

Wakes of Wind Turbines

Image above: The above photograph shows the turbulence field behind the Horns Rev offshore wind turbines. Horns Rev is located in the North Sea, 14 kilometers west of Denmark. Photographer Christian Steiness. From (http://wattsupwiththat.com/2011/04/28/the-wind-turbine-albedo-effect/).

STANFORD
AERONAUTICS &
ASTRONAUTICS

Spread of radioactive seawater from the Fukushima disaster

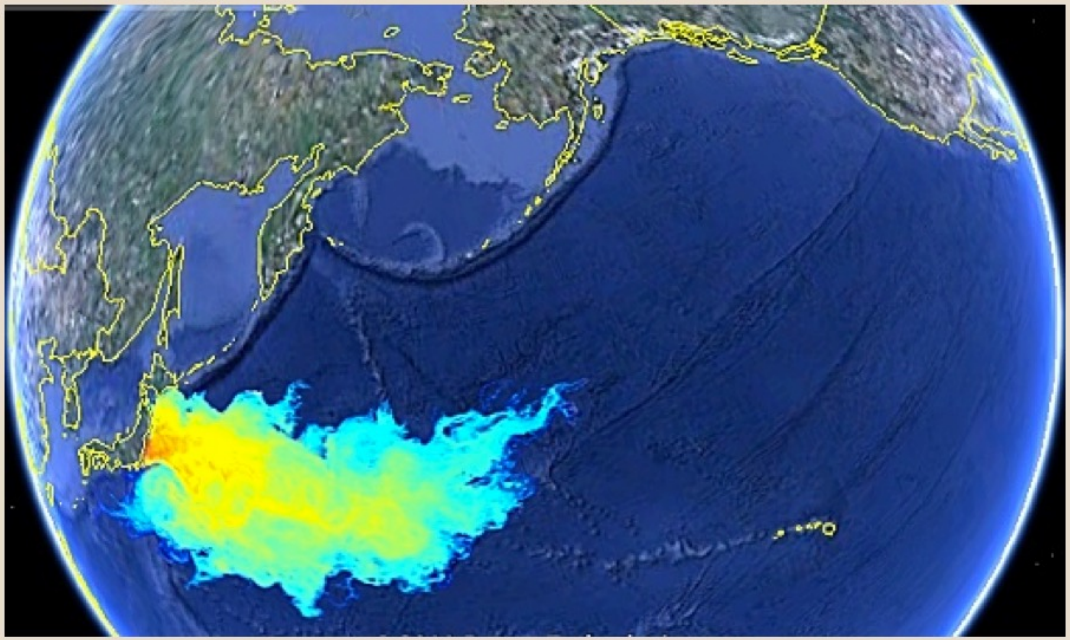

Image above: 8/11/11 simulation of radioactive seawater dispersed from Fukushima nears Hawaii. From (http://www.xydo.com/toolbar/27327691-asr_ltd_-_fukushima_radioactive_seawater_plume_dispersal_simulation). Note - users can zoom and rotate orientation of simulation.

STANFORD
AERONAUTICS &
ASTRONAUTICS

Turbulent kinetic energy spectrum

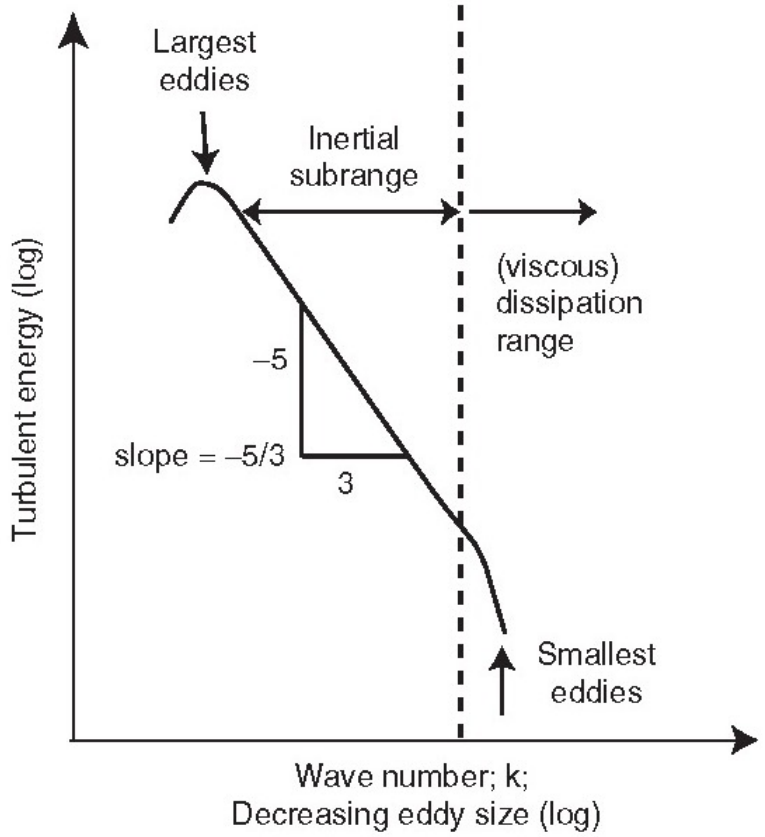

STANFORD AERONAUTICS & ASTRONAUTICS

The turbulent kinetic energy (TKE) equation

Momentum and continuity equations

$$\frac{\partial u^i}{\partial x^i} = 0$$

$$\frac{\partial u^i}{\partial t} + \frac{\partial}{\partial x^j}\left(u^i u^j + \frac{p}{\rho}\delta^{ij} - 2\nu s^{ij} \right) = 0$$

$$s^{ij} = \frac{1}{2}\left(\frac{\partial u^i}{\partial x^j} + \frac{\partial u^i}{\partial x^j} \right)$$

Kinetic energy equation - project the momentum equation onto the velocity vector

$$u^i \frac{\partial u^i}{\partial t} + u^i \frac{\partial}{\partial x^j}\left(u^i u^j + \frac{p}{\rho}\delta^{ij} - 2\nu s^{ij} \right) = 0$$

$$u^i \frac{\partial u^i}{\partial t} = \frac{\partial\left(\frac{u^i u^i}{2} \right)}{\partial t}$$

$$u^i \frac{\partial u^i u^j}{\partial x^j} = u^i u^j \frac{\partial u^i}{\partial x^j} + u^i u^i \frac{\partial u^j}{\partial x^j} = u^i u^j \frac{\partial u^i}{\partial x^j}$$

$$\frac{\partial\left(\frac{u^i u^i}{2} u^j \right)}{\partial x^j} = u^i u^j \frac{\partial u^i}{\partial x^j} + \frac{u^i u^i}{2}\frac{\partial u^j}{\partial x^j} = u^i u^j \frac{\partial u^i}{\partial x^j}$$

$$\frac{\partial\left(\frac{u^i u^i}{2} \right)}{\partial t} + \frac{\partial}{\partial x^j}\left(\frac{u^i u^i}{2} u^j + \frac{p}{\rho} u^j - 2\nu u^i s^{ij} \right) + 2\nu \frac{\partial u^i}{\partial x^j} s^{ij} = 0$$

Kinetic energy dissipation

$$2\nu \frac{\partial u^i}{\partial x^j} s^{ij} =$$

$$2\nu\left(\frac{1}{2}\left(\frac{\partial u^i}{\partial x^j} + \frac{\partial u^j}{\partial x^i} \right) + \frac{1}{2}\left(\frac{\partial u^i}{\partial x^j} - \frac{\partial u^j}{\partial x^i} \right) \right) s^{ij} =$$

$$2\nu\left(s^{ij} + \omega^{ij} \right) s^{ij} = 2\nu s^{ij} s^{ij}$$

STANFORD AERONAUTICS & ASTRONAUTICS

Decompose the flow into a mean and fluctuating part.

$$\text{TKE} \equiv \frac{\overline{u'^i u'^i}}{2}$$

A

$$\frac{\partial\left(\frac{\overline{u}^i\overline{u}^i}{2}+\frac{\overline{u'^i u'^i}}{2}\right)}{\partial t}+\frac{\partial}{\partial x^j}\left(\frac{\overline{u}^i\overline{u}^i}{2}\overline{u}^j+\frac{\overline{u'^i u'^i}}{2}\overline{u}^j+\overline{u'^i u'^i}\overline{u}^i+\frac{\overline{u'^i u'^i u'^j}}{2}+\overline{u}^j\frac{\overline{p}}{\rho}+\frac{\overline{u'^j p'}}{\rho}-2\nu\left(\overline{u}^i\overline{s}^{ij}+\overline{u'^i s'^{ij}}\right)\right)+2\nu\left(\overline{s}^{ij}\overline{s}^{ij}+\overline{s'^{ij}s'^{ij}}\right)=0$$

Project the mean momentum equation onto the mean velocity vector

$$\overline{u}^i\frac{\partial\overline{u}^i}{\partial t}+\overline{u}^i\overline{u}^j\frac{\partial\overline{u}^i}{\partial x^j}+\overline{u}^i\frac{\partial\overline{u'^i u'^j}}{\partial x^j}+\frac{\partial}{\partial x^j}\left(\frac{\overline{p}\overline{u}_j}{\rho}\right)-2\nu\overline{u}^i\frac{\partial\overline{s}^{ij}}{\partial x^j}=0$$

$$\overline{u}^i\frac{\partial\overline{s}_{ij}}{\partial x^j}=\frac{\partial}{\partial x^j}\left(\overline{u}^i\overline{s}^{ij}\right)-\overline{s}^{ij}\overline{s}^{ij}$$

$$\frac{\partial\left(\frac{\overline{u}^i\overline{u}^i}{2}\right)}{\partial t}+\overline{u}^j\frac{\partial\left(\frac{\overline{u}^i\overline{u}^i}{2}\right)}{\partial x^j}+\overline{u}^i\frac{\partial\overline{u'_i u'_j}}{\partial x^j}+\frac{\partial}{\partial x^j}\left(\frac{\overline{p}\overline{u}^j}{\rho}\right)-2\nu\frac{\partial}{\partial x^j}\left(\overline{u}^i\overline{s}^{ij}\right)+2\nu\overline{s}^{ij}\overline{s}^{ij}=0$$

B

$$\frac{\partial\left(\frac{\overline{u}^i\overline{u}^i}{2}\right)}{\partial t}+\frac{\partial}{\partial x^j}\left(\frac{\overline{u}^i\overline{u}^i}{2}\overline{u}_j+\overline{u'_i u'_j}\overline{u}_i+\frac{\overline{p}\overline{u}_j}{\rho}-2\nu\overline{u}_i\overline{s}_{ij}\right)-\overline{u'_i u'_j}\frac{\partial\overline{u}_i}{\partial x^j}+2\nu\overline{s}_{ij}\overline{s}_{ij}=0$$

Subtract B from A .

STANFORD AERONAUTICS & ASTRONAUTICS

Subtract B from A .

The turbulent kinetic energy (TKE) transport equation is

TKE production

$$\frac{\partial\left(\frac{\overline{u'^i u'^i}}{2}\right)}{\partial t}+\frac{\partial}{\partial x^j}\left(\frac{\overline{u'^i u'^i}}{2}\bar{u}^j+\frac{\overline{u'^i u'^i u'^j}}{2}+\frac{\overline{u'^j p'}}{\rho}-2\nu\left(\overline{u'^i s'^{ij}}\right)\right)+\overline{u'^i u'^j}\frac{\partial \bar{u}^i}{\partial x^j}+2\nu\left(\overline{s'^{ij}s'^{ij}}\right)=0$$

TKE dissipation

Consider homogeneous shear flow

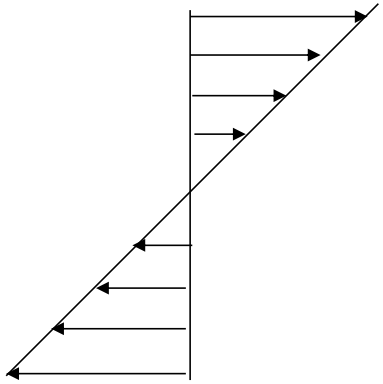

$$\bar{u}=(ky,0,0)$$

All gradients of correlations are zero

The important implication of all this is that the dissipation term is comparable to all the other terms in the kinetic energy balance despite the fact that is is multiplied by the kinematic viscosity

Conclusion: fluctuating rates of strain are very large!

$$2\nu\left(\overline{s'^{ij}s'^{ij}}\right)=-\overline{u'^i u'^j}\frac{\partial \bar{u}^i}{\partial x^j} \qquad \varepsilon=2\nu\overline{s'^{ij}s'^{ij}}$$

Dissipation of TKE equals production of TKE

STANFORD
AERONAUTICS &
ASTRONAUTICS

Fine scale motions - The Taylor Microscale

Using the scaling relation (13.11) that comes from the turbulent kinetic energy equation, we can write

$$\varepsilon \propto \frac{u_0^3}{\delta}, \tag{13.40}$$

which can be rearranged to read

$$\sqrt{\overline{s'^{ik}s'^{ki}}} \propto \frac{u_0}{\delta}\left(\frac{u_0\delta}{2\nu}\right)^{1/2} \tag{13.41}$$

This affirms the statement made earlier that the instantaneous rates of strain are larger than mean rates of strain by a factor proportional to the square root of the Reynolds number. Given u_0 and δ, this result can be used to estimate, the size of the microscale motions that contribute the largest fluctuating strain rates and therefore the bulk of the energy dissipation in a one-parameter flow.

We now define a new length scale, λ, called the *Taylor microscale*, that, when associated with u_0, can account for turbulent kinetic energy dissipation [13.11], [13.13]:

$$\varepsilon \propto \nu\left(\frac{u_0^2}{\lambda^2}\right). \tag{13.42}$$

Combining (13.42) with (13.40) leads to the following estimates for the Taylor microscale:

$$\frac{\lambda}{\delta} \propto \frac{1}{(R_\delta)^{1/2}}, \qquad \lambda \propto (\nu(t-t_0))^{1/2}. \tag{13.43}$$

According to this estimate, there is always some eddying motion in the flow which has a characteristic length that varies like $\sqrt{\nu t}$ and is independent of the governing parameter M. In a similar vein note that the velocity gradients of the large-scale motion vary according to

$$\frac{u_0}{\delta} \propto \frac{1}{t-t_0} \qquad (t > t_0), \tag{13.44}$$

which is also independent of M. In a sense the large-scale gradients constitute a clock that can be used to date the evolution of the flow just as in the case of the laminar round jet.

STANFORD
AERONAUTICS &
ASTRONAUTICS

Fine scale motions - The Kolmogorov Microscale

Now let's define new length *and* velocity scales that can account for dissipation of TKE. These are the velocity and length scales defined by Kolmogorov [13.14]. See also the discussion of Kolmogorov theory in References [13.15] and [13.16]. The Kolmogorov scales can be regarded as motions that constitute the lower limit for instability – motions with a characteristic Reynolds number of order one. Let

$$\varepsilon \propto \nu\left(\frac{\upsilon^2}{\eta^2}\right), \qquad \frac{\upsilon\eta}{\nu} \approx 1. \tag{13.45}$$

Equation (13.45) can be used in conjunction with (13.12) to generate the following estimates of the Kolmorgorov velocity and length scales:

$$\frac{\eta}{\delta} \propto \frac{1}{(R_\delta)^{3/4}}, \qquad \eta \propto \nu^{3/4} M^{-1/2m} (t - t_0)^{3/4 - k/2} \tag{13.46}$$

and

$$\frac{\upsilon}{u_0} \propto \frac{1}{(R_\delta)^{1/4}}, \qquad \upsilon \propto \nu^{1/4} M^{1/2m} (t - t_0)^{k/2 - 3/4}. \tag{13.47}$$

In a sense, the Taylor and Kolmogorov microscales bracket the range of scales that contribute the bulk of the dissipation of TKE in the flow. At scales larger than the Taylor microscale the turbulent motion is considered to be essentially inviscid. At the smallest scale are the Kolmogorov microscales with a local Reynolds number of order one. The fine-scale gradients over the whole range of dissipating motions vary according to

$$\frac{u_0}{\lambda} \propto \frac{\upsilon}{\eta} \propto \nu^{-1/2} M^{1/m} (t - t_0)^{k - 3/2}. \tag{13.48}$$

Note that k=3/2 would correspond to a flow where the velocity gradients do not vary in time, Very strong forcing!

Turbulent kinetic energy spectrum (again)

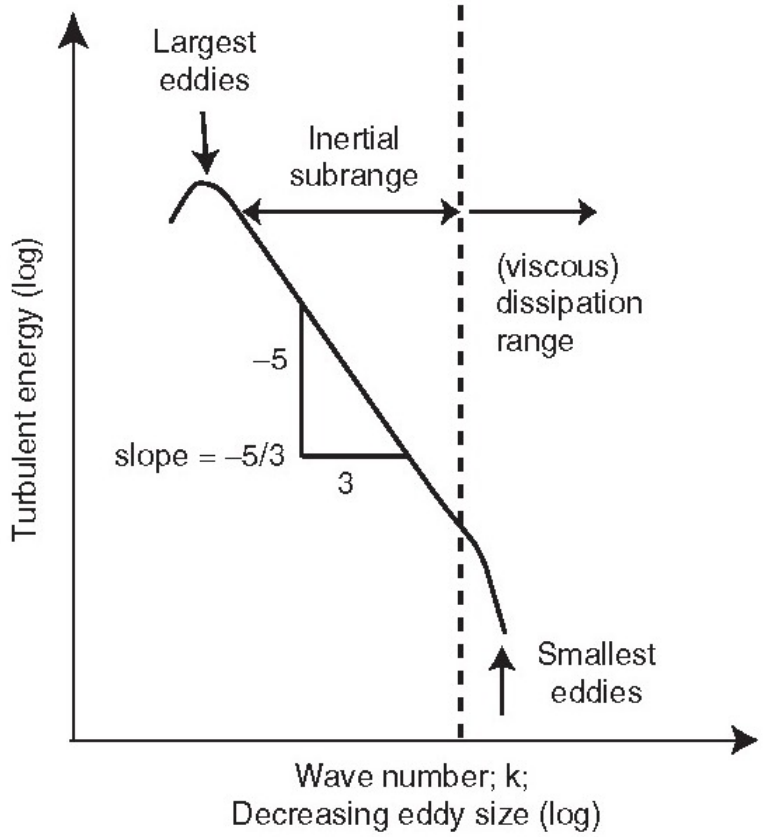

STANFORD
AERONAUTICS &
ASTRONAUTICS

Scaling the inertial subrange

Assume the governing parameter is

$$M = \varepsilon \propto u_0^3/\delta \tag{13.49}$$

with units $\hat{u}_0^3/\hat{\delta} = L^2T^{-3}$ and exponent $k = \frac{3}{2}$.

$$\delta \propto \varepsilon^{1/2}(t - t_0)^{3/2}, \qquad u_0 \propto \varepsilon^{1/2}(t - t_0)^{1/2} \tag{13.50}$$

$$R_\delta \propto (t - t_0)^2, \qquad \lambda \propto (t - t_0)^{1/2}, \qquad \eta \propto (t - t_0)^0. \tag{13.51}$$

The wavenumber of an eddy is essentially the inverse of its scale.

$$\kappa \propto 1/\delta. \tag{13.52}$$

STANFORD
AERONAUTICS &
ASTRONAUTICS

The TKE per unit wavenumber should scale as

$$E(\kappa) \propto \frac{u_0^2}{1/\delta} \propto \varepsilon^{3/2}(t - t_0)^{5/2}. \tag{13.53}$$

$$t - t_0 \propto \frac{\delta^{2/3}}{\varepsilon^{1/3}} \propto \frac{\kappa^{-2/3}}{\varepsilon^{1/3}}. \tag{13.54}$$

$$E(\kappa) \propto \varepsilon^{2/3}\kappa^{-5/3}. \tag{13.55}$$

This is the scaling of TKE first postulated by Kolmogorov in 1941
and seems to agree with measurements in high Reynolds number flows.

STANFORD
AERONAUTICS &
ASTRONAUTICS

Measurements of spectra carried out in the boundary layer on the roof of the large wind tunnel at NASA Ames

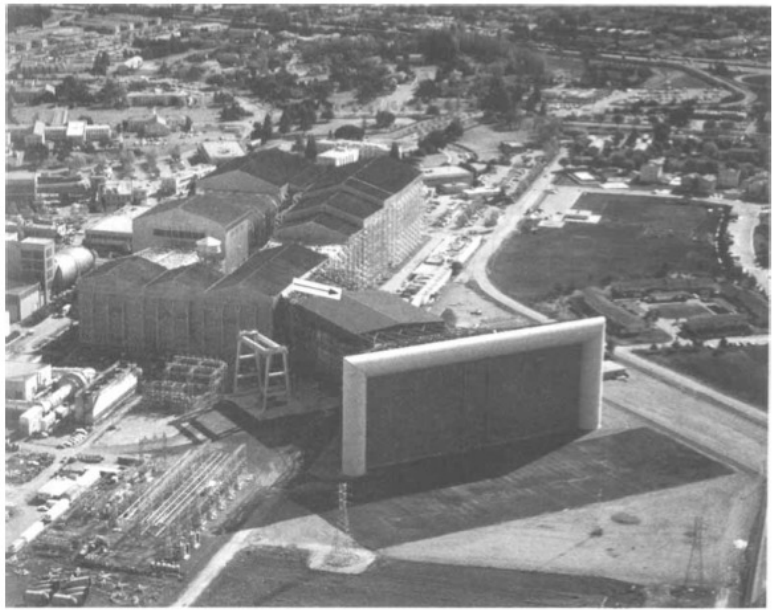

FIGURE 1. An aerial view of the Full-Scale Aerodynamics Facility at NASA Ames Research Center, showing the intake to the 80 × 120 foot test section. The arrow shows our measurement location in the attic.

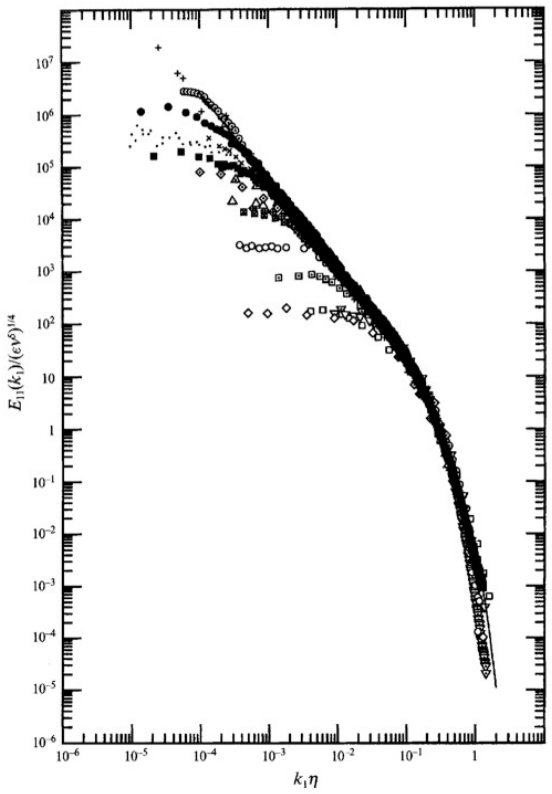

FIGURE 9. Kolmogorov's universal scaling for one-dimensional longitudinal power spectra. The present mid-layer spectra for both free-stream velocities are compared with data from other experiments. This compilation is from Chapman (1979), with later additions. The solid line is from Pao (1965). R_λ: □, 23 boundary layer (Tielman 1967); ◇, 23 wake behind cylinder (Uberoi & Freymuth 1969); ▽, 37 grid turbulence (Comte-Bellot & Corrsin 1971); ▽, 53 channel centreline (Kim & Antonia (DNS) 1991); ⊡, 72 grid turbulence (Comte-Bellot & Corrsin 1971); ○, 130 homogeneous shear flow (Champagne *et al.* 1970); ⊠, 170 pipe flow (Laufer 1954); ⊕, 282 boundary layer (Tielman 1967); ◈, 308 wake behind cylinder (Uberoi & Freymuth 1969); △, 401 boundary layer (Sanborn & Marshall 1965); △, 540 grid turbulence (Kistler & Vrebalovich 1966); ×, 780 round jet (Gibson 1963); ·, 850 boundary layer (Coantic & Favre 1974); +, ~ 2000 tidal channel (Grant *et al.* 1962); ⊙, 3180 return channel (CAHI Moscow 1991); ●, 1500 boundary layer (present data, mid-layer: $U_e = 50$ m s^{-1}); ■, 600 boundary layer (present data, mid-layer: $U_e = 10$ m s^{-1}).

STANFORD
AERONAUTICS &
ASTRONAUTICS

Astronomers see Kolmogorov scaling in their data

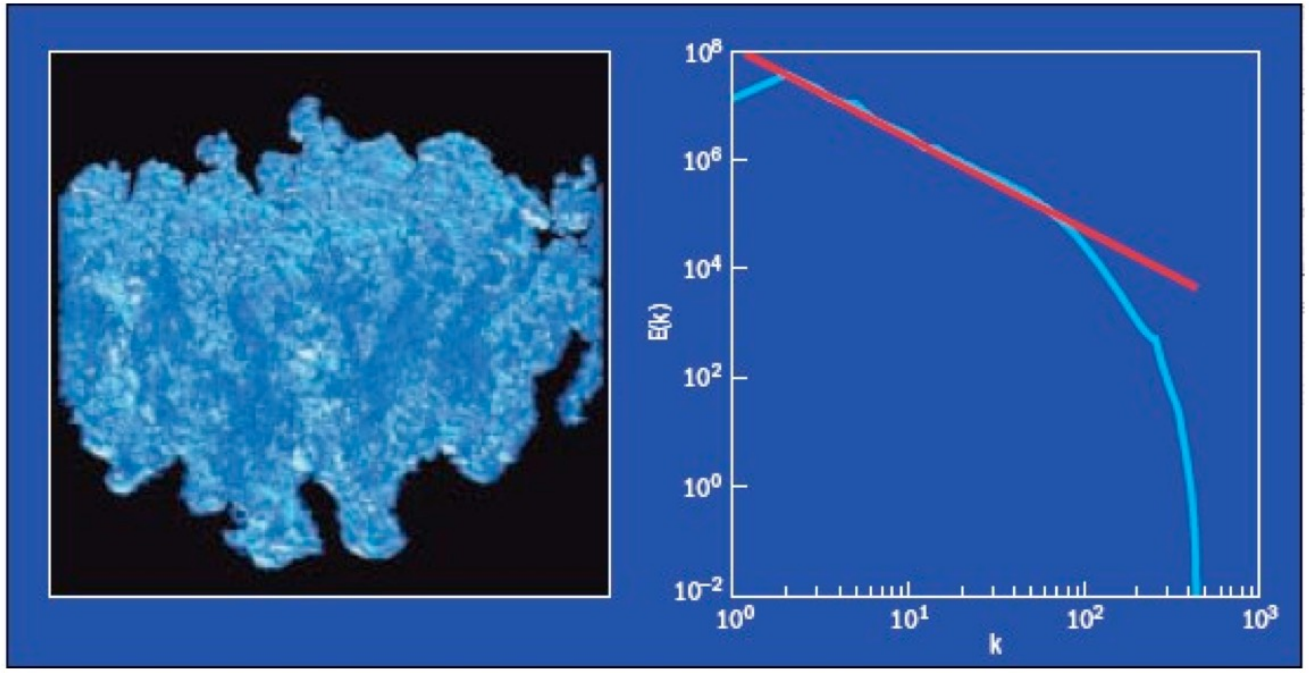

Figure 10. Image of a three-dimensional Rayleigh–Taylor unstable flame in a Type Ia supernova and the computed kinetic energy spectrum (blue curve) exhibiting the classical $k^{5/3}$ decay (red line).

STANFORD
AERONAUTICS & ASTRONAUTICS

Concluding Remarks

The similarity rules developed in this lecture can be used to estimate length, velocity and time scales in a variety of basic flows.

Even flows where the initial region may be dominated by several length scales, as is the case with the origins of jets and wakes, the downstream region often follows the scaling of a single governing parameter. If k>1/2 the range of scales increases continuously. If k<1/2 viscosity eventually dominates the motion.

The case k=1/2 is special in that the governing parameter has units commensurate with the kinematic viscosity. In this case, the Reynolds number is constant, and the problem is invariant under the basic dilation group of the Navier Stokes equations. Virtually all exact solutions of the NS equations fall into this class.

In the next lecture we will we will use these methods to determine the nature of transition in an impulsively started jet.

Table 13.1. *Various one-parameter shear flows and the units of the associated governing parameter.*

Flow	Invariant	M	Units	k
	Jetlike flows			
Plane mixing layer	Velocity difference	U_0	LT^{-1}	1
Plane jet	2-D momentum flux	$U_0^2\delta$	L^3T^{-2}	$\frac{2}{3}$
Round jet	3-D momentum flux	$U_0^2\delta^2$	L^4T^{-2}	$\frac{1}{2}$
Radial jet	3-D momentum flux	$U_0^2\delta^2$	L^4T^{-2}	$\frac{1}{2}$
Vortex pair	2-D impulse	$U_0\delta^2$	L^3T^{-1}	$\frac{1}{3}$
Vortex ring	3-D impulse	$U_0\delta^3$	L^4T^{-1}	$\frac{1}{4}$
Plane plume	2-D buoyancy flux	U_0^3	L^3T^{-3}	1
Round plume	3-D buoyancy flux	$U_0^3\delta$	L^4T^{-3}	$\frac{3}{4}$
Plane thermal	2-D buoyancy	$U_0^2\delta$	L^3T^{-2}	$\frac{2}{3}$
Round thermal	3-D buoyancy	$U_0^2\delta^2$	L^4T^{-2}	$\frac{1}{2}$
Line vortex	Circulation	$U_0\delta$	L^2T^{-1}	$\frac{1}{2}$
Diverging channel	Area flux	$U_0\delta$	L^2T^{-1}	$\frac{1}{2}$
Vortex-sheet rollup	Apex $\alpha; n = 1/(2-\alpha/\pi)$	$U_0^2\delta^{2-n}$	$L^{3-n}T^{-1}$	$1/(3-n)$
	Wakelike flows			
Plane wake	(2-D drag)/U_∞	$U_0\delta$	L^2T^{-1}	$\frac{1}{2}$
Round wake	(3-D drag)/U_∞	$U_0\delta^2$	L^3T^{-1}	$\frac{1}{3}$
Plane jet in cross flow	(2-D mom. flux)/U_∞	$U_0\delta$	L^2T^{-1}	$\frac{1}{2}$
Round jet in cross flow	(3-D mom. flux)/U_∞	$U_0\delta^2$	L^3T^{-1}	$\frac{1}{3}$
Plane plume in cross flow	(2-D buoy. flux)/U_∞	U_0^2	L^2T^{-2}	1
Round plume in cross flow	(3-D buoy. flux)/U_∞	$U_0^2\delta$	L^3T^{-2}	$\frac{2}{3}$
Grid turb. initial decay	Saffman invariant	$U_0^2\delta^3$	L^5T^{-2}	$\frac{2}{5}$
Grid turb. initial decay	Loitsianski invariant	$U_0^2\delta^5$	L^7T^{-2}	$\frac{2}{7}$

STANFORD
AERONAUTICS &
ASTRONAUTICS

Main References

Cantwell, Brian J., *Introduction to Symmetry Analysis,* Cambridge University Press, Cambridge Texts in Applied Mathematics, 2002.

Cantwell, Brian J., *Organized Motion in Turbulent Flow,* Annual Reviews of Fluid Mechanics 13: 457-515, 1981.

Brown, G. L. and Roshko, A. 1974. On density effects and large structure in turbulent mixing layers. *J. Fluid Mech.* **64** (4):775–816.

Glezer, A. and Coles, D. E. 1990. An experimental study of a turbulent vortex ring. *J. Fluid Mech.* **211**:243–284.

Cantwell, B. J. 1999. Reynolds number invariance and the dilation group of turbulence, in *Modern Group Analysis VII*, Proceedings of the International Conference at the Sophus Lie Conference Center, Nordfjordeid, Norway, June 30 to July 5, pp. 41–52.

Cantwell, B., Coles, D. and Dimotakis, P. 1978. Structure and entrainment on the plane of symmetry of a turbulent spot. *J. Fluid Mech*. **87**:641–672.

Saddoughi, S.G. and S. V. Veeravalli 1994. Local isotropy in turbulent boundary layers at high Reynolds number. J. Fluid Mech. **268**: 333-372